TRANSPLANT INTERNATIONAL

Transplant International ISSN 0934-0874

ORIGINAL ARTICLE

Cyclosporine-mediated allograft fibrosis is associated with micro-RNA-21 through AKT signaling

Jianguo Chen,[1] Anna Zmijewska,[1] Degui Zhi[2] and Roslyn B. Mannon[1]

1 Division of Nephrology, Department of Medicine, University of Alabama at Birmingham, Birmingham, AL, USA
2 Department of Biostatistics, School of Public Health, University of Alabama at Birmingham, Birmingham, AL, USA

Keywords
cyclosporine, fibrosis, microRNA, nephrotoxicity, signaling, transplantation.

Correspondence
Roslyn B. Mannon MD, University of Alabama at Birmingham, 1900 University Boulevard, THT 643, Birmingham, AL 35294, USA.
Tel.: 205 934 7220;
fax: 205 975 0102;
e-mail: rmannon@uab.edu

Conflicts of Interest
The authors have declared no conflicts of interest.

Received: 3 June 2014
Revision requested: 6 July 2014
Accepted: 21 September 2014
Published online: 30 October 2014

doi:10.1111/tri.12471

Summary

Calcineurin inhibitors (CNIs) are potent immunosuppressants with associated long-term nephrotoxicity mediated by tubular epithelial cell injury and arterial vasoconstriction. We hypothesized that CNI-induced renal injury is regulated by specific microRNAs (miRNAs). In this study, we found that 46 miRNAs were significantly altered in human proximal tubular epithelial cells (HPTECs) following exposure to cyclosporine A (CsA), particularly miR-21 (5.47 ± 0.47-fold versus vehicle, $P = 0.002$). This increase was accompanied by alterations in epithelial–mesenchymal transformation (EMT) markers including vimentin (2.80 ± 0.28-fold; $P = 0.03$), S100A4 (2.29 ± 0.29-fold; $P = 0.04$), and α-SMA (5.0 ± 0.31-fold; $P = 0.03$). Notably, transfection of HPTECs with miR-21 precursor also resulted in significant induction of EMT-associated genes, which were inhibited by a single-stranded nucleic acid inhibitor of miR-21. miR-21 induction resulted in a rapid increase of phosphorylated AKT and downregulation of PTEN. While CsA induces SMAD7 downregulation and TGF-β1 upregulation in HPTECs, such changes were independent of miR-21. Moreover, there was no effect on ERK phosphorylation. We confirmed these changes using a mouse model of CsA toxicity. Collectively, our results suggest that miR-21 mediates CsA nephrotoxicity via PTEN/AKT signaling pathway. Further exploration into the epigenetic response to CsA exposure may provide new therapeutic targets to ameliorate CsA nephrotoxicity.

Introduction

MicroRNAs (miRNAs) are a family of small noncoding RNAs with the length of 21–25 nucleotides. They regulate the expression of various cellular proteins by translational repression or mRNA degradation by binding to target sites in the 3'-untranslated regions of protein-coding transcripts [1,2]. Approximately 2000 miRNA genes have been identified in the human genome [3] associated with numerous cellular and developmental processes, including intracellular signaling pathways and organ morphogenesis [2,4,5]. Aberrant expression of miRNAs is closely associated with initiation and progression of pathophysiologic processes including diabetes, cancer [6], cardiovascular disease [7,8], renal disease and ischemia reperfusion injury [7,9], and liver disease [6].

Recent studies indicate that microRNA-21 (miR-21) is associated with organ fibrosis in the kidney, lung, liver, and heart [6–14]. For example, miR-21 is upregulated in the experimental mice lung fibrosis as well as in lung biopsy samples in human Idiopathic pulmonary fibrosis [10,11]. These increased miR-21 levels are associated with epithelial–mesenchymal transition in pulmonary epithelial cells [15]. In the mouse, kidneys with unilateral ureteral obstruction express higher levels of miR-21 than unobstructed mice [8], and blockade of miR-21 in this model attenuates fibrosis [11,14]. Finally, in humans, renal allografts with severe interstitial fibrosis have enhanced expression of miR-21 compared to those without fibrosis [7,8].

Moreover, recipients with allograft fibrosis have higher circulating miR-21 levels [8]. However, the effect of immunosuppression was not analyzed.

In organ transplantation, the calcineurin inhibitors (CNIs), cyclosporine A (CsA), and tacrolimus, revolutionized the field due to their potent immunosuppressive properties [16]. However, their nephrotoxic effects on the kidney leading to IF/TA have limited their success in the long-term. Prior studies of CsA-induced nephrotoxicity demonstrated direct effects of CsA on proximal tubular cells (PTECs) [17] with associated phenotypic change characteristic of epithelial-to-mesenchymal transition (EMT) [18–20], leading to renal interstitial fibrosis [20]. However, the expression patterns and the role of miRNAs in CsA nephrotoxicity are as yet unknown. Therefore, determining the roles of miRNAs may suggest important new directions to ameliorate CsA toxicity in the kidney.

In this study, we found that CsA exposure *in vitro* induces phenotypic changes coincident with miR-21 induction. Moreover, miR-21 is overexpressed in the kidneys of mice with CsA nephrotoxicity. CsA-induced miR-21 expression is associated with AKT phosphorylation with downregulation of PTEN in treated PTECs. Further, inhibition of miR-21 significantly reduces CsA-induced EMT gene upregulation. Taken together, these results suggest that miR-21 is an important mediator in CsA nephrotoxicity and a potential target for developing novel therapeutics in treating CsA-induced renal fibrosis.

Materials and methods

Reagents

Cyclosporine A (Alexis Biochemicals, CA, USA) was prepared as a 6 mM stock solution in 100% ethanol. Stock solutions of 1 mM wortmannin (WM) and 10 mM U0126 (Cell signaling, Beverly, MA, USA) were prepared in dimethyl sulfoxide (DMSO). Cells were preincubated for 1 h with 1 μM WM or 10 μM U0126 prior to treatment with 6 μM CsA either alone or in combination.

Cell culture

Human renal proximal tubular epithelial cells (PT2 cells: a gift from Dr. Anthony Jevnikar, University of Western Ontario, CAN; [21]) were cultured in a 1:1 mixture of Dulbecco's modified Eagle's medium and Ham's F12 medium (DMEM/F12) with 10% FBS, 100 U/ml penicillin, and 100 mg/ml streptomycin and cultured in a humidified atmosphere of 5% CO_2. Subconfluent cell lines were serum deprived for 16–24 h prior to being subjected to vehicle (Veh), or 6 μM CsA treatment. 0.25% trypsin was used to detach the cells from the culture flask.

Experimental mouse model of CsA nephrotoxicity

We utilized a previously reported mouse model [22–24]. Briefly, male ICR mice (Charles River, Wilmington, MA, USA), weighing 30–40 g, were housed in individual cages and placed on a very low-salt diet (0.01% sodium diet, Teklad Premier, Madison, WI, USA) for 7 days prior to treatment and continued on this diet throughout the treatment period. CsA provided by Novartis Research (East Hanover, NJ, USA) was diluted in olive oil to a final concentration of 15 mg/ml. In the vehicle group, mice received a daily subcutaneous injection of olive oil, 1 mg/kg for 1–8 weeks. In the CsA group, mice received a daily subcutaneous injection of CsA, 50 mg/kg, for 1–8 weeks. Four to six mice were used in each treatment group, and at each time point, they were sacrificed and total RNA was isolated from the kidneys. The animal protocol was approved by the NIH Institutional Animal Care and Use Committee (IACUC).

miRNA and transient transfection

To alter miR-21 levels in PTECs, PTECs were cultured to 50–60% confluence and transfected with either (i) the miR-21 precursor ('Pre-21'), (ii) the negative control of precursor miRNA ('Pre-Ctrl'), which consisted of a scrambled sequence of the Pre-miR-21 molecule, (iii) the antagomir to miR-21 ('Anti-21'), or (iv) the negative control of the inhibitor miRNA ('Anti-Ctrl'), which consisted of a scrambled sequence of the anti-miR-21 molecule (Ambion, Forster City, CA, USA). Transfection was performed using a solution of lipofectamine 2000 transfecting reagent (Invitrogen, Carlsbad, CA, USA) and serum-free OPTI-MEM 1 medium according to the manufacturer's instruction. After room temperature incubation 5 min with lipofectamine, each oligomer was then added to the above mixture (total volume is 500 μl), vortexed, and incubated at room temperature for 20 min. The mixture was added to dishes containing 1.5 ml of fresh media with 10% FBS. 10, 25, and 50 nM of oligomer were tested, with a transfection efficiency of 75–80%. The final concentration of oligomer used was 25 nM. After 24 h of transfection at 37 °C, the media was replaced with fresh media containing 0.5% FBS overnight before treatment with the appropriate test conditions. The specific protein expression was analyzed in the cells by Western blotting, and levels of mRNA expression in the cells were analyzed by RT-PCR.

Validation of the anti-miR-21 inhibitor

1×10^4 PTECs per well were preplated in white-walled flat clear bottom 96-well plates (Corning, Union City, CA, USA). After overnight incubation, the cells were transfected with 40 ng of the miR-21 luciferase vector with or without anti-miR-21 inhibitor (25, 50, and 100 nM per well).

Nontransfected cells, cells transfected with luciferase vector without insert of miR-21 sequence were used as controls. Cells transfected with β-Gal vector were used for normalization. A master mix of the Lipofectamine 2000 (0.2 μl Lipofectamine 2000 + 9.8 μl OPTI-MEM/well) was made and incubated at room temperature for 5 min, followed by incubation with vectors/inhibitors for another 20 min, which was added to preplated cells. After 24 h, luciferase activity was measured using ABI Dual-light system (Applied Biosystems, Forster City, CA, USA).

TaqMan® microRNA array analysis

Human PTECs (2×10^5 cells per well) were cultured in 6-well plates and treated with 6 μM CsA or vehicle in duplicate. At 6 h, cells were harvested, and total RNA was isolated using Trizol reagent (Invitrogen). cDNAs were generated by TaqMan® microRNA Reverse Transcription Kit (Applied Biosystems) according to manufacturer's instructions. Resulting cDNAs were used for miRNA analysis by quantitative real-time PCR using TaqMan® microRNA arrays (Human MicroRNA A Cards v2.0; Applied Biosystems). This array interrogated 377 known human miRNAs. RT-PCR reactions were performed according to the manufacturer's instructions. Briefly, 500 ng of total RNA obtained from cells was reverse transcribed using Megaplex RT Primers and the TaqMan miRNA reverse transcription kit in a total of 7.5 μl volume. qRT-PCR array was performed on ABI 7900HT fast real-time PCR system and a TaqMan Universal PCR Master Mix with 400 ng cDNA input per fill port of each card. The expression levels of miRNA were normalized to endogenous control U6.

Quantitative-PCR analysis of gene expression

Total RNAs were isolated from cells using Trizol reagent (Invitrogen). cDNAs were generated by Superscript III first-strand cDNA synthesis system (Invitrogen) according to the manufacturer's protocol. Resulting cDNAs were used for quantitative real-time PCR using TaqMan mRNA assay (Applied Biosystems). Thermal cycling was performed on an ABI 7900HT fast real-time PCR system (Applied Biosystems). The expression levels of mRNA were normalized to endogenous control 18 s. The relative miRNA or mRNA level was calculated by the $2^{-\Delta\Delta Ct}$ method and expressed as fold relative to vehicle treatment.

In situ hybridization of mouse kidneys for miR-21

In situ hybridization (ISH) was performed on FFPE sections using Exiqon double-DIG LNA™ microRNA probes (Exiqon A/S, Vedback, DK) and Exiqon microRNA ISH kit (#90002) [25]. In brief, the slides were deparaffinized in xylene and ethanol solutions at room temperature, incubated with 15 μg/ml proteinase-K for 10 min at 37 °C, washed twice in PBS, dehydrated in new ethanol solutions, and air-dried on clean paper towels for 15 min. Slides were then hybridized in incubation chambers overnight at 53 °C in an oven using 50 nM double-DIG LNA™ miR-21 probe diluted with microRNA ISH buffer. After hybridization, slides were washed in SSC buffer followed by incubation with AP-conjugated anti-Dig antibody 2 h at room temperature. After washing three times with PBST, the sections were developed with NBT/BCIP (Roche) for 4 h at room temperature and visualized under microscopy with light blue staining being positive.

Western blot analysis

After the experiments were performed, cells were lysed using ice-cold lysis buffer (20 mM Tris–HCl, 150 mM NaCl, 1% Triton X-100, 0.5% sodium deoxycholate, 0.1% SDS, 200 μM PMSF, 2 mM EDTA, 1 mM sodium orthovanadate, protease inhibitor cocktail, and 50 mM sodium fluoride). The lysate was placed on ice for 20 min and then centrifuged at 10 000 *g* for 10 min at 4 °C. Protein concentration of the supernatant was measured using Bio-Rad Lowry protein assay. Equal amounts of protein were subjected to SDS/PAGE using 10% polyacrylamide gels. Gels were blotted onto PVDF membrane, and proteins were detected using anti-ERK (9107), anti-phospho-ERK (9106), anti-phospho-AKT (9271), anti-AKT (9272), anti-PTEN antibodies (9559) from Cell Signaling Technology, followed by an appropriate HRP-conjugated secondary antibody. The visualization of the blots was carried out by the use of an enhanced chemiluminescence kit (GE Healthcare Bio-Sciences, Pittsburgh, PA, USA and Millipore Corporation, Billerica, MA, USA). GAPDH (anti-GAPDH, MAB374, Millipore) was used as the loading control.

TGF-β1 ELISA

Active TGF-β1 protein in CsA-treated PTECs media was measured by TGF-β1 ELISA method (Duo set Development System, R&D Systems, Minneapolis, MN, USA) according to the manufacturer's instructions. Protein concentration of the media was measured using Bio-Rad Lowry protein assay. The final TGF-β1 concentration values were normalized to total protein level.

Statistical analysis

Data are presented as mean ± SEM. Statistical differences among groups were determined by one-way ANOVA followed by Student–Newman–Keuls' test or Turkey–Kramer test. Between two groups, statistical significance was assessed using 2-tailed student's *t*-test. The differences

were considered significant if the P value was < 0.05. Two-tailed student's t-test was used for the miRNA array data. The dendrogram of miRNAs was generated by JMP PRO 10.0.2 (SAS, Cary, NC, USA) with the Ward's minimum variance hierarchical clustering.

Results

CsA treatment changes the morphology of human renal proximal tubular epithelial cells (PTECs) and induces EMT gene expression

Proximal tubular epithelial cells were treated for 48 h with 6 μM CsA, and cell morphology was assessed by phase contrast microscopy. Compared to vehicle-treated cells, CsA-treated cells developed epithelial disruption exhibited by elongated shape, the development of lamellipodiae, and a high degree of cell detachment (Fig. 1a). Indeed, consistent with prior observations [26–28], exposure of human proximal tubular epithelial cells with CsA results in significant morphological changes with a fibroblastic phenotype (Fig. 1a). Paralleling the morphological changes, CsA treatment induces significant increases in gene expression of mesenchymal markers S100A4 (2.29 ± 0.29-fold; $P = 0.04$), α-SMA (5.0 ± 0.31-fold; $P = 0.03$), and vimentin (2.80 ± 0.28-fold; $P = 0.03$) compared to vehicle-treated cells (Fig. 1b). Concomitantly, E-cadherin (E-cad) mRNA (0.34 ± 0.07-fold) was significantly downregulated by CsA treatment ($P = 0.01$). These results demonstrate that CsA induces a phenotypic transition from an epithelial tubular cell to a mesenchymal phenotype.

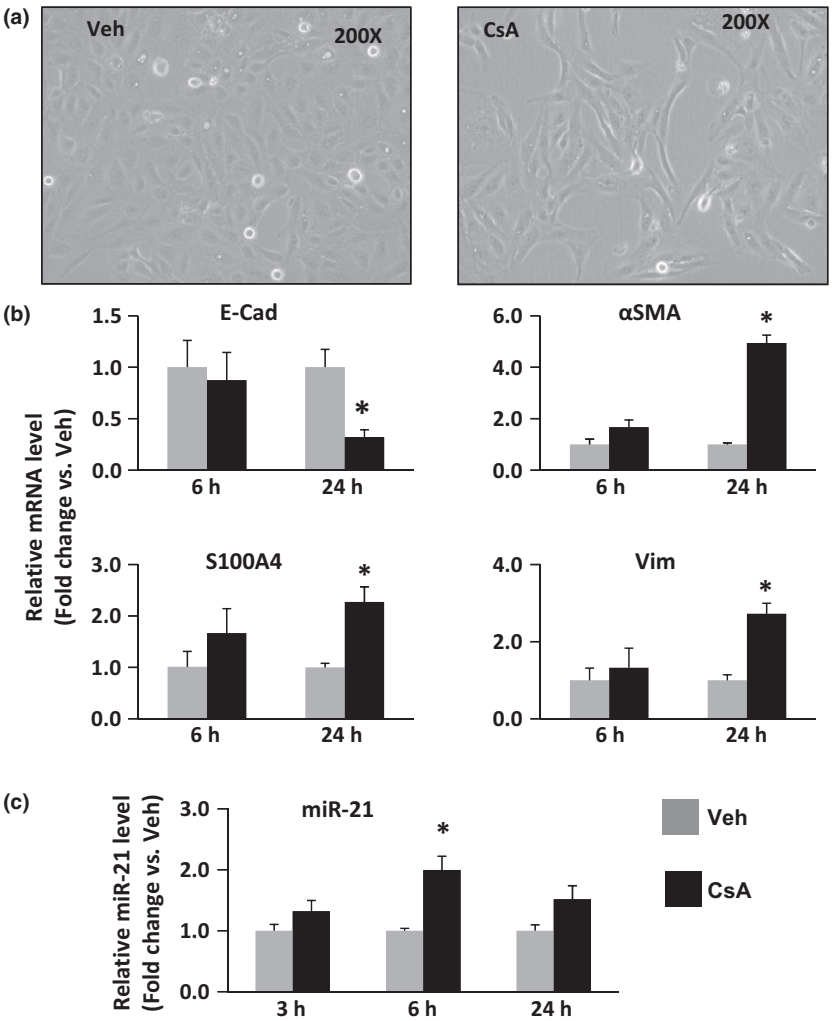

Figure 1 CsA treatment induces morphologic changes in HPTECs. (a) HPTECs were exposed with CsA 6 μM for 48 h. Compared to vehicle-treated cells (Veh), CsA-treated cells demonstrated epithelial disruption, and morphological changes consistent with a fibroblastic phenotype. (b) PTECs were treated with 6 μM CsA for 6 and 24 h. Cells were collected and total RNAs were extracted. Real-time PCR was used to analyze the mRNA expression of epithelial–mesenchymal transformation (EMT) markers S100A4, α-SMA, E-cadherin and vimentin. (c) For miR-21 expression, cells were exposed for 3, 6, and 24 h. Data represent the mean of 4 experiments performed in triplicate. $*P < 0.05$, compared to vehicle-treated cells.

(a)

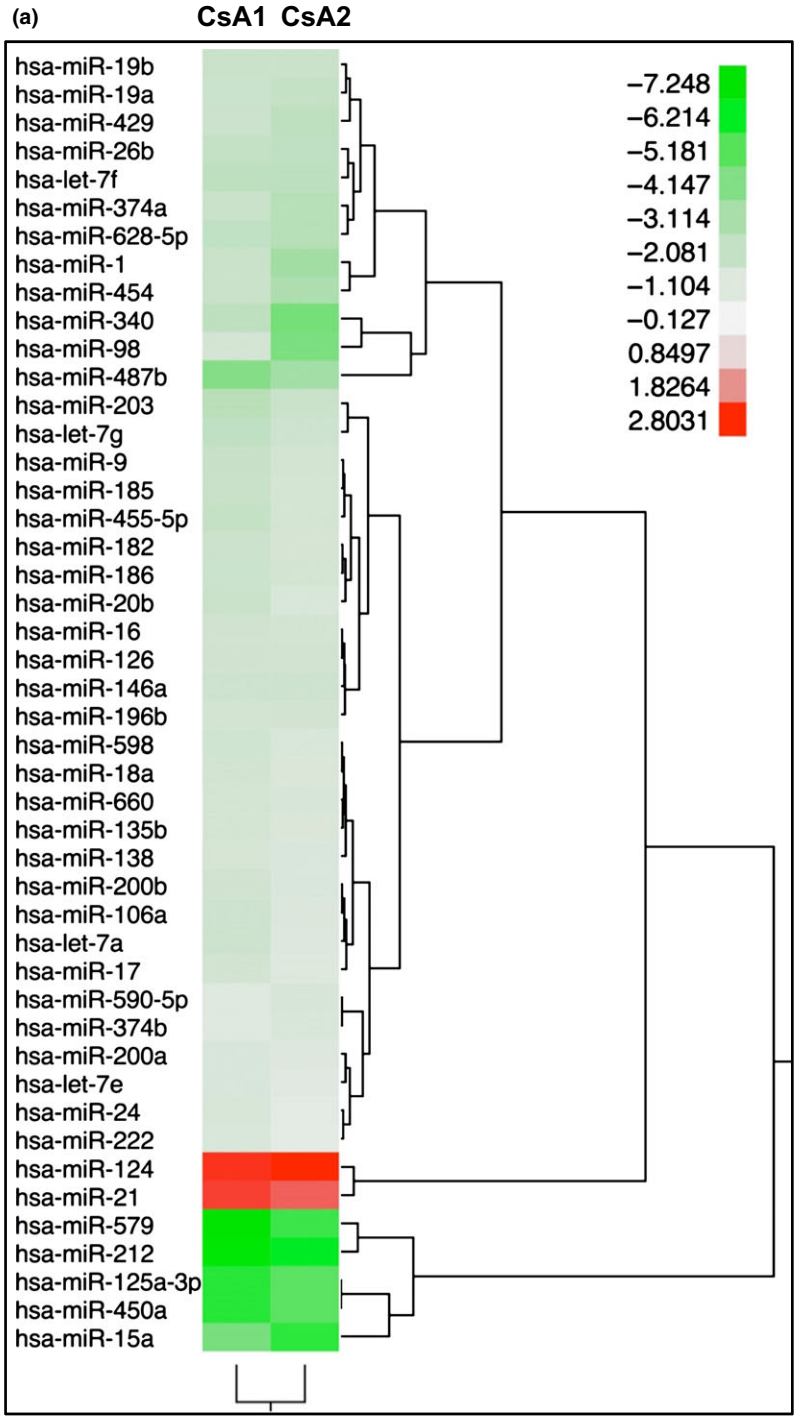

(b)

miRNA	Fold change
hsa-miR-19b	0.25
hsa-miR-19a	0.25
hsa-miR-429	0.23
hsa-miR-26b	0.22
hsa-let-7f	0.19
hsa-miR-374a	0.21
hsa-miR-628-5p	0.19
hsa-miR-1	0.18
hsa-miR-454	0.19
hsa-miR-340	0.12
hsa-miR-98	0.20
hsa-miR-487b	0.08
hsa-miR-203	0.22
hsa-let-7g	0.25
hsa-miR-9	0.28
hsa-miR-185	0.29
hsa-miR-455-5p	0.28
hsa-miR-182	0.32
hsa-miR-186	0.31
hsa-miR-20b	0.32
hsa-miR-16	0.31
hsa-miR-126	0.31
hsa-miR-146a	0.30
hsa-miR-196b	0.32
hsa-miR-598	0.35
hsa-miR-18a	0.36
hsa-miR-660	0.36
hsa-miR-135b	0.37
hsa-miR-138	0.39
hsa-miR-200b	0.36
hsa-miR-106a	0.37
hsa-let-7a	0.37
hsa-miR-17	0.40
hsa-miR-590-5p	0.43
hsa-miR-374b	0.43
hsa-miR-200a	0.43
hsa-let-7e	0.46
hsa-miR-24	0.46
hsa-miR-222	0.48
hsa-miR-124	6.75
hsa-miR-21	5.47
hsa-miR-579	0.01
hsa-miR-212	0.01
hsa-miR-125a-3p	0.02
hsa-miR-450a	0.02
hsa-miR-15a	0.03

Figure 2 miRNA array analysis of human PTECs exposed to cyclosporine A. (a) Total RNA was isolated from duplicate wells of human PTECs exposed to either vehicle or cyclosporine (CsA1, CsA2) for 6 h. microRNA array analysis was performed as described in the methods and unsupervised hierarchical clustering is shown. (b) Fold values for miRNAs expressed in human PTECs that are ≥ twofold compared to vehicle and statistically significant from vehicle ($P < 0.05$). Expression of 44 miRNAs was significantly reduced while only miR-124 and miR-21 were significantly increased following CsA treatment.

miR-21 expression is upregulated in CsA-treated human PTECs

To identify potential miRNAs and their role in CsA-induced EMT, we performed miRNA expression profiling in CsA-treated human PTECs using TaqMan® human microRNA array, which contains 384 TaqMan MicroRNA Assays enabling accurate quantitation of 377 human miRNAs. At 6 h, we found 122 miRNAs expressed at least two-fold compared to vehicle treatment. Of these, 46 miRNAs were significantly altered in their expression following CsA exposure compared with vehicle-treated PTECs ($P < 0.05$), the vast majority downregulated (Fig. 2). Only 2 were upregulated significantly: miR-21 (5.47 ± 0.42-fold; $P = 0.0014$) and miR-124 (6.75 ± 0.23; $P = 0.002$). To further confirm the array data, we analyzed expression of miR-21 by TaqMan microRNA assay. Consistent with the miRNA array analysis, the expression of miR-21 was significantly increased by 2.00 ± 0.23-fold ($P = 0.001$; Fig. 1c) compared to vehicle treatment.

miR-21 expression is upregulated in the kidneys of mice with CsA toxicity

Because of recent data implicating miR-21 in kidney fibrosis [7,14], we focused our investigation on its potential role in CsA-mediated renal injury. We tested the relevance of our findings *in vivo* by characterizing miR-21 expression in a mouse model of chronic cyclosporine nephrotoxicity previously reported by Bennett and colleagues [29,30]. Animals were studied at 2, 4, and 8 weeks of CsA exposure. These kidneys demonstrate tubular injury in the first 2 weeks of exposure and subsequently develop interstitial fibrosis and tubular atrophy by 8 weeks of treatment (data not shown). We found that miR-21 expression in the kidney was significantly induced in the first 2 weeks of CsA treatment (2.11 ± 0.13-fold compared to vehicle; $P = 0.02$), which returns to baseline after that time point (Fig. 3a). Following this upregulation, at 4 weeks, we see a significant induction of S100A4 (2.40 ± 0.16-fold compared to vehicle; $P = 0.001$) and vimentin (2.37 ± 0.39-

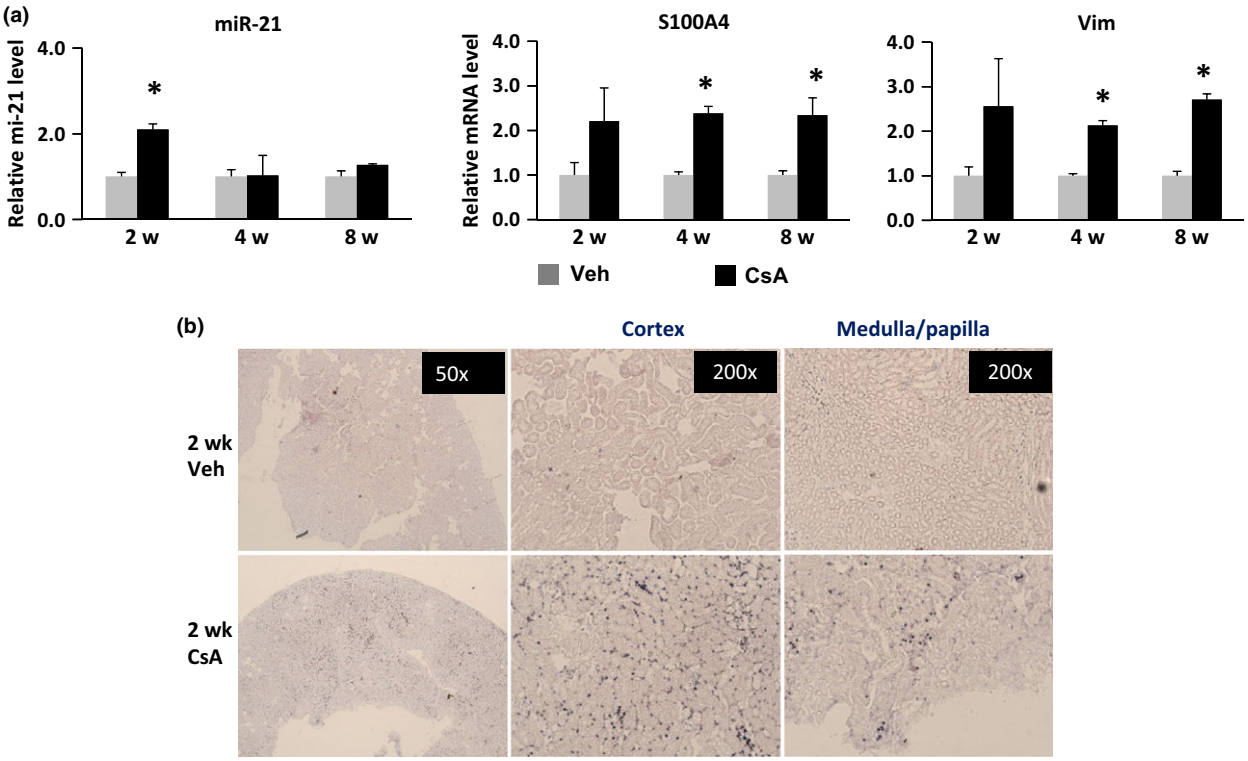

Figure 3 (a) miR-21 and epithelial–mesenchymal transformation (EMT) gene expression are induced in a mouse model of CsA nephrotoxicity. Mice ($n = 40$ in each group) received a daily subcutaneous injection of either vehicle (olive oil 1 mg/kg) or CsA (50 mg/kg) for 1–8 weeks. Mice ($n = 4$–6/group/week) were sacrificed at 2, 4, and 8 weeks after treatment, and total RNAs from mice kidneys were isolated. Compared to vehicle-treated mice (Veh), miR-21 expression in the kidney was significantly induced in the first 2 weeks of CsA treatment, followed by gene expression of S100A4 and vimentin that was significantly increased at 4 and 8 weeks of CsA treatment (*$P < 0.05$, compared to vehicle(Veh)-treated group, $n = 4$–6). (b) *In situ* hybridization for miR-21 in the kidney of CsA-nephrotoxic mice. At 2 weeks post-treatment, CsA treatment demonstrated substantial induction of miR-21 in both cortex and medulla of the kidney in epithelial cells compared to Veh treatment. Scrambled sequence was used as a negative control and is not shown.

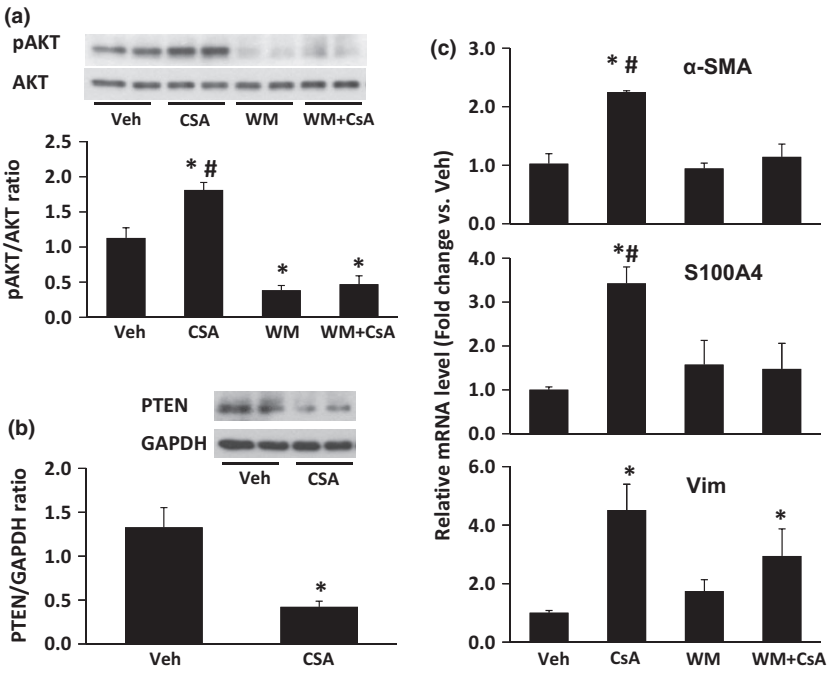

Figure 4 CsA induces AKT Phosphorylation and downregulates PTEN expression. (a) PTECs were pretreated with either vehicle (Veh) or 1 μM WM for 1 h, followed by 6 μM CsA treatment for 1 h. Western analysis was carried out using the same amount of protein extracts. A representative blot from three experiments preformed in duplicate is shown. *$P < 0.05$, compared to vehicle-treated group or WM alone and #$P < 0.05$ compared to WM + CsA. (b) PTEN expression is suppressed after 1 h exposure to 6 μM CsA. Blot is representative of three experiments performed in duplicate. *$P < 0.05$ compared to vehicle-treated group. (c) mRNA expressions for mesenchymal markers expressed in PTECs induced by CsA are inhibited by WM pretreatment. *$P < 0.05$, compared to vehicle-treated group or WM alone and #$P < 0.05$ compared WM + CsA group.

fold compared to vehicle; $P = 0.04$), prior to the development of fibrosis. This expression remained persistently elevated at 8 weeks of CsA treatment (2.13 ± 0.11-fold and 2.72 ± 0.13-fold, respectively compared to vehicle) (Fig. 3a). Thus, in a preclinical model of CsA nephrotoxicity, miR-21 upregulation precedes expression of profibrotic genes expression and is associated with tissue fibrosis.

In situ hybridization was also performed on kidney sections from nephrotoxic mice at 2 weeks after treatment with CsA, when detection by PCR was most significant. miR-21 was detected throughout the kidney in both cortex and medulla (Fig. 3b). Localization was primarily in tubules and not in vessels or glomeruli, which are unaffected by this toxicity. Moreover, expression was substantially higher in CsA-treated mice than that seen in vehicle-treated mice.

Induction of miR-21 by CsA results in AKT phosphorylation and downregulation of PTEN signaling

We next investigated the specific signaling pathways associated with miR-21 induction and the associated phenotypic changes in our cell line. Recent studies have demonstrated that expression of miR-21 increases cell proliferation, migration, and invasion through modulating PTEN [31–33]. Moreover, PTEN is an antagonist of phosphatidylinotidol 3-kinase (PI3K) by dephosphorylation of phosphatidylinositol 3, 4, 5-trisphosphate (PIP3), the upstream regulator AKT [34–36]. Whether the PTEN or the AKT signaling pathways are activated by CsA remains to be elucidated.

Exposure to CsA rapidly induces upregulation of AKT phosphorylation within 1 h (Fig. 4a) and downregulated PTEN expression (Fig. 4b). Pretreatment with WM, a specific inhibitor of PI3 Kinase, suppressed CsA-induced AKT activation (Fig. 4a). Moreover, WM pretreatment significantly suppressed CsA-induced expression of α-SMA (1.14 ± 0.22-fold vs. 2.24 ± 0.02-fold; $P = 0.03$ compared to CsA alone) and S100A4 (1.48 ± 0.58 vs. 3.34 ± 0.37; $P = 0.04$ compared to CsA alone), with a substantial but not significant reduction in vimentin (2.95 ± 0.92 vs. 4.51 ± 0.88; $P = 0.35$ compared to CsA alone) (Fig. 4c). Thus, CsA-mediated mesenchymal changes are associated with AKT activation and PTEN downregulation and specific inhibition of this pathway suppresses the expression of mesenchymal markers.

Overexpression of miR-21 induces EMT gene expression via upregulation of AKT phosphorylation and reduction of PTEN

We next evaluated the relationship between CsA-mediated miR-21 induction, mesenchymal change gene expression, and AKT signaling. We first evaluated the effects of overexpression by miR-21 on gene expression for mesenchymal markers (Fig. 5a), as described in the methods. Compared to a negative control precursor miRNA (Pre-Ctrl), transfection with precursor miRNA-21 (Pre-21) led to significant upregulation of S100A4 (3.14 ± 0.90-fold; $P = 0.04$) and vimentin (2.04 ± 0.30-fold; $P = 0.02$) expression and increased α-SMA (2.31 ± 0.69-fold; $P = 0.09$). Furthermore, overexpression of miR-21 induces significant upregulation of AKT phosphorylation (Fig. 5b) and reduction of PTEN at 3 h post exposure (Fig. 5c). Thus, miR-21 induces similar responses in gene expression as seen with CsA treatment.

We next determined the strength of this association by determining whether blocking miR-21 in PTECs would affect CsA-induced EMT and PTEN/AKT signaling. To this end, PTECs were transfected with miR-21 inhibitor (Anti-21) or the negative control of inhibitor miRNA (Anti-Ctrl) for 48 h prior to CsA treatment. Anti-21 is a chemically modified, single-stranded nucleic acid designed to specifically bind to and inhibit endogenous miR-21 molecules. As shown in Fig. 6a, transfection with Anti-Ctrl had no effect on CsA-induced AKT phosphorylation. However, transfection with Anti-21 significantly blocked phosphorylation to a level similar to vehicle exposed cells. Similarly, transfection with miR-21 inhibitor reversed the suppression of PTEN expression seen after CsA exposure (Fig. 6b), to a level similar to vehicle-treated cells.

The effect of Anti-21 on EMT gene expression is shown in Fig. 6c. Compared to Anti-Ctrl and CsA-treated cells, miR-21 inhibitor treatment decreased CsA-induced gene expression of α-SMA by 45% (5.10 ± 0.57-fold vs 9.56 ±

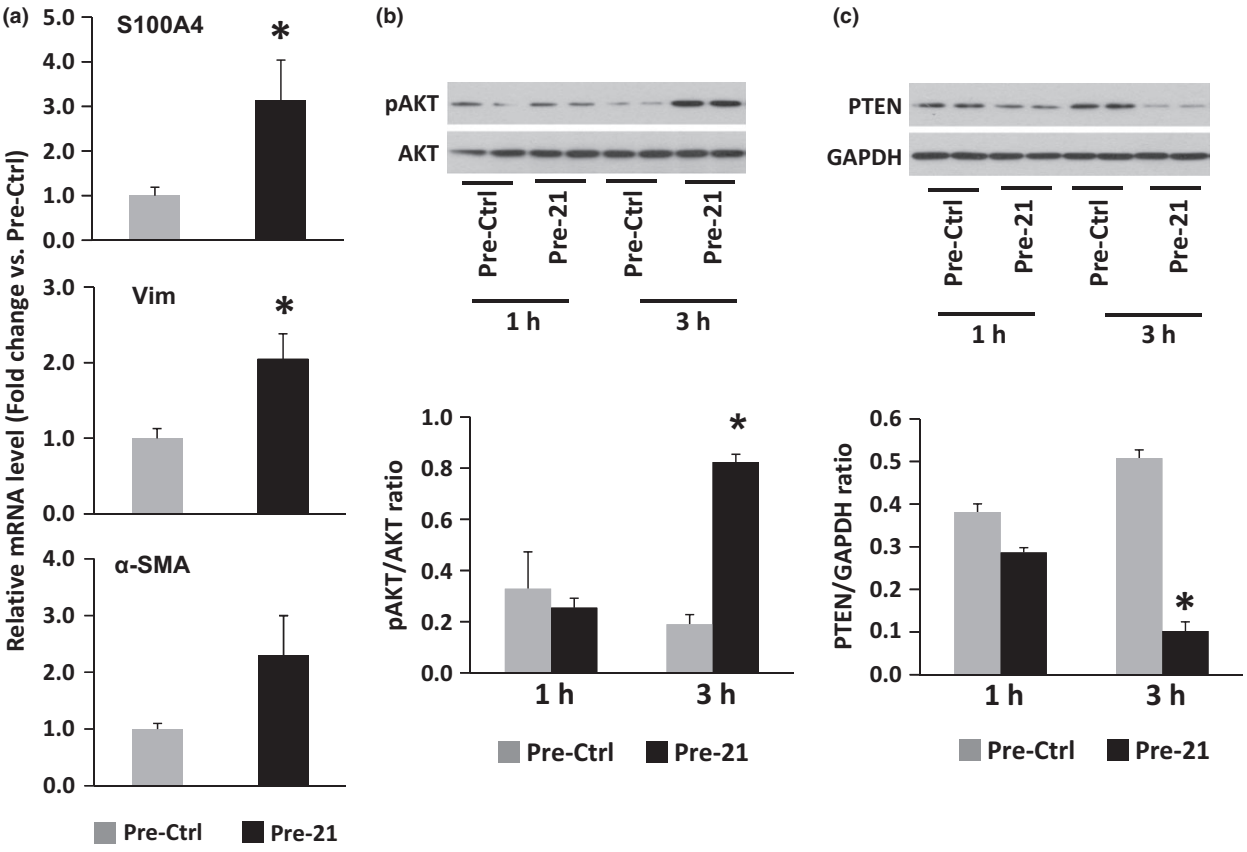

Figure 5 (a) Overexpression of miR-21 induces epithelial–mesenchymal transformation (EMT) gene expression. (a) Human PTECs were transfected with precursor miR-21 (Pre-21) or pre-miR-21 negative control (Pre-Ctrl). Cells were collected and subjected to qRT-PCR for EMT gene expression 48 h after transfection. Transfection with precursor significantly increased transcription of S100A4 and vimentin. (b) Overexpression of miR-21 treatment upregulates AKT phosphorylation. Cells were collected 1 and 3 h after transfection with Pre-21. The total protein was extracted and subjected to Western blot assay. *$P < 0.05$, compared to the pre-miRNA negative control. (c) Overexpression of miR-21 treatment downregulates PTEN. *$P < 0.05$, compared to the pre-miRNA negative control.

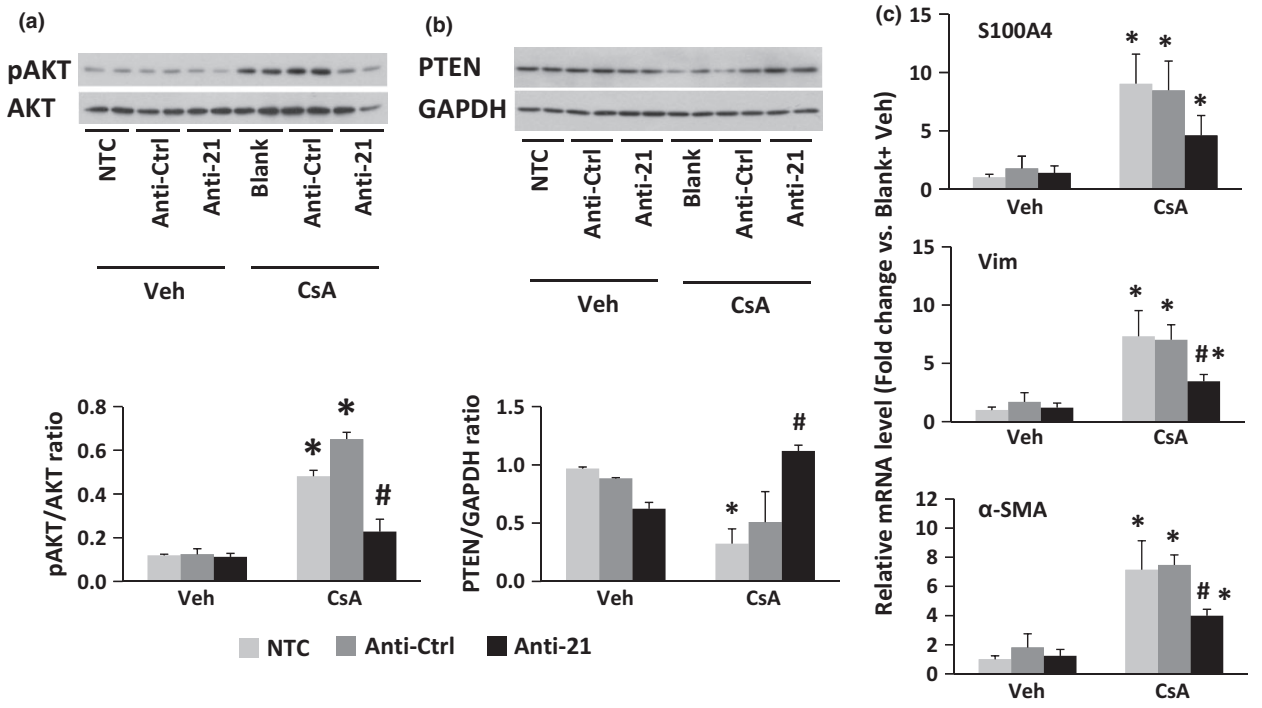

Figure 6 Inhibition of miR-21 reduces CsA-induced AKT activation and epithelial–mesenchymal transformation (EMT) gene expression. PTECs were transfected with miR-21-inhibitor (Anti-21) or a negative control of the inhibitor miRNA (Anti-Ctrl) for 48 h, followed by 6 μM CsA treatment for 1 h. A nontransfected control is shown for comparison (NTC). (a) Anti-21 significantly reduced CsA-induced AKT activation, to levels seen with vehicle treatment. (b) Anti-21 treatment releases the suppression of CsA on PTEN expression. (c) Anti-21 significantly reduces CsA-induced expression of mesenchymal genes α-SMA, vimentin, and S100A4. *$P < 0.05$ compared to vehicle-treated groups, #$P < 0.05$ compared to nontransfected control and Anti-Ctrl treated with CsA.

0.88-fold, $P = 0.005$), vimentin by 53% (3.89 ± 0.66-fold vs 7.91 ± 1.45-fold, $P = 0.045$), and S100A4 by 35%, although this was not significant ($P = 0.25$) (Fig. 6c). These results further demonstrate that downregulation of miR-21 not only affects AKT activation and PTEN suppression, but dampens the CsA-stimulated expression of mesenchymal genes, demonstrating an important functional role for miR-21 in CsA nephrotoxicity.

CsA-induced miR-21 signaling is independent of ERK activation

Thum *et al.* [12] demonstrated that miR-21 levels are selectively increased in fibroblasts of the failing heart, augmenting ERK–MAP kinase activity through inhibition of sprouty homologue 1 (Spry1) in cardiac hypertrophy. ERK activation also follows stimulation with CsA in other non-epithelial cell types [37,38]. To this end, we evaluated the potential of ERK activation in renal epithelial cells. Treatment of PTECs with 6 μM CsA led to a rapid phosphorylation of ERK with a peak at 15 min (Fig. 7a), which was specifically blocked by U-0126, the MAPK-specific inhibitor (Fig. 7b). However, inhibition of miR-21 did not affect CsA-induced ERK activation (Fig. 7c). These results suggest that CsA-induced expression of miR-21 and associated mesenchymal changes in epithelial cells are not mediated by ERK signaling.

Alteration of TGF-β/SMAD7 signaling in CsA-induced miR-21 and phenotypic changes

A number of signaling pathways have been implicated in CsA nephrotoxicity [20,27,39,40] and in particular, TGF-β [41]. Further, in the lung, miR-21 regulates fibrosis by altering SMAD7 and thus TGF-β function by directly reducing SMAD7 in epithelial cells [11]. Conversely, TGF-β itself may induce miR-21 expression in renal epithelial cells, and blockade of SMAD3 signaling is critical in this pathway [42]. Thus, we evaluated the contribution of TGF-β in our *in vitro* studies. Consistent with previous studies [27,28], CsA treatment of PTECs induces a significant increase in active TGF-β1 mRNA expression and TGF-β1 protein release in the media compared to vehicle treatment at 24 and 48 h after CsA exposure, with a significant decrease in SMAD7 expression compared to vehicle treatment at 6 h after CsA exposure (data not shown). However, inhibition of miR-21 with Anti-21 treatment did not block CsA-induced TGFβ transcription (Fig. 8a and b) nor

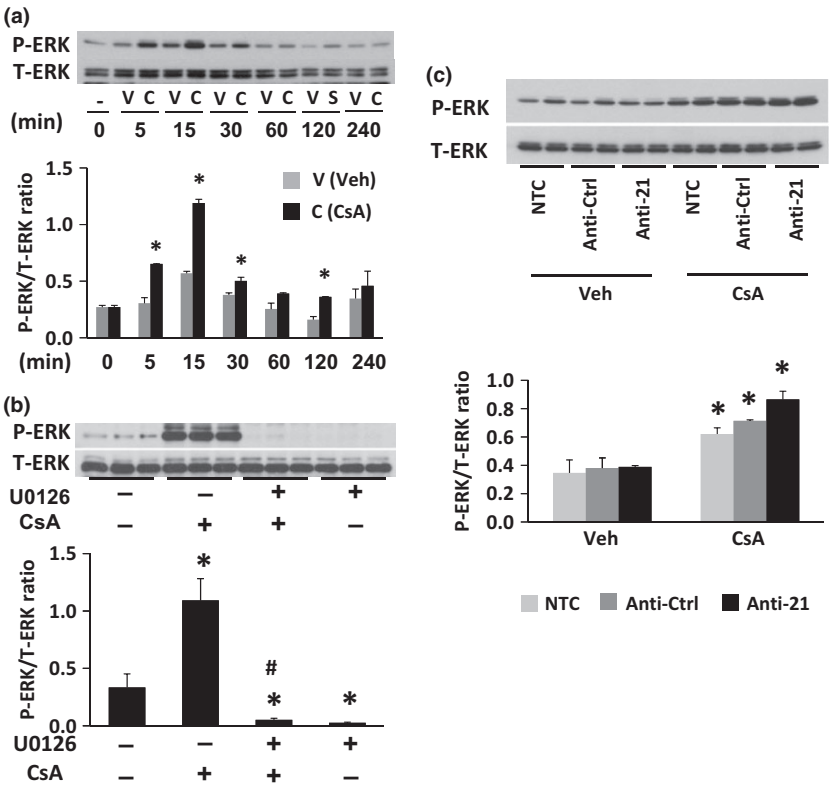

Figure 7 CsA-induced ERK activation is independent of miR-21 induction. (a) CsA treatment of PTECs results in rapid phosphorylation of ERK. A representative blot from three experiments performed in duplicate is shown. (b) CsA-induced phosphorylation was blocked by U0126, the MAPK-specific inhibitor. PTECs were pretreated with either vehicle or 10 μM U0126 for 1 h, followed by 6 μM CsA treatment for 15 min. A representative blot from three experiments performed in duplicate is shown. *$P < 0.05$ compared to vehicle-treated cells; #$P < 0.05$ compared to CsA-treated cells. (c) Inhibition of miR-21 function by Anti-21 has no effect on ERK signaling mediated by CsA treatment. PTECs were transfected with Anti-21 or negative control of inhibitor miRNA (Anti-Ctrl) for 48 h, followed by 6 μM CsA treatment for 15 min. Nontransfected control (NTC) is shown for comparison. A representative blot is shown for ERK expression. *$P < 0.05$, compared to vehicle-treated groups.

affect TGFβ release into the media (Fig. 8c and d). Nor did Anti-21 treatment significantly restore CsA-induced SMAD7 downregulation (Fig. 8e). Thus, CsA-mediated miR-21 signaling and phenotypic changes appear to be relatively independent of the effects on TGF-β and suggest a novel pathway for CsA injury and fibrosis.

Discussion

Renal transplantation provides a substantial benefit to those with end-stage renal disease with improved morbidity and mortality compared to dialysis modalities. While short-term graft survival is excellent, long-term graft survival continues to be problematic. Late graft loss is multifactorial and includes both immune- and nonimmune-mediated injuries [43]. In this regard, there are a lack of defined therapies and insights into mechanisms of chronic injury. miRNAs have been identified as potential regulators of gene expression and have been identified in mediating native kidney disease [14,34,44]. In transplantation, miRNAs might provide an opportunity not only to identify therapeutic targets but to better enhance our understanding about graft loss. Indeed, recent studies suggest that miRNAs may play critical roles such as regulating acute rejection in heart allografts [45] and kidney allografts [46], in recipients with chronic allograft nephropathy (defined as interstitial fibrosis and tubular atrophy) [7,8,47] and in ischemia/reperfusion injury of the kidney [9,48]. Further studies are needed to determine their potential impact in immune monitoring particularly in long-term outcomes.

The chronic use of the CNI cyclosporine A has been associated with nephrotoxicity, histologically characterized by interstitial fibrosis, myofibroblast formation, and matrix deposition [16,49]. Here, we demonstrate for the first time that renal tubular epithelium exposure to CsA has a profound effect on miRNA expression. Not unlike other transplant-related studies [7,9], there were a large number of dysregulated miRNAs following a simple manipulation. This unique profile and differential expression included only 2 miRNAs that were significantly elevated, miR-124

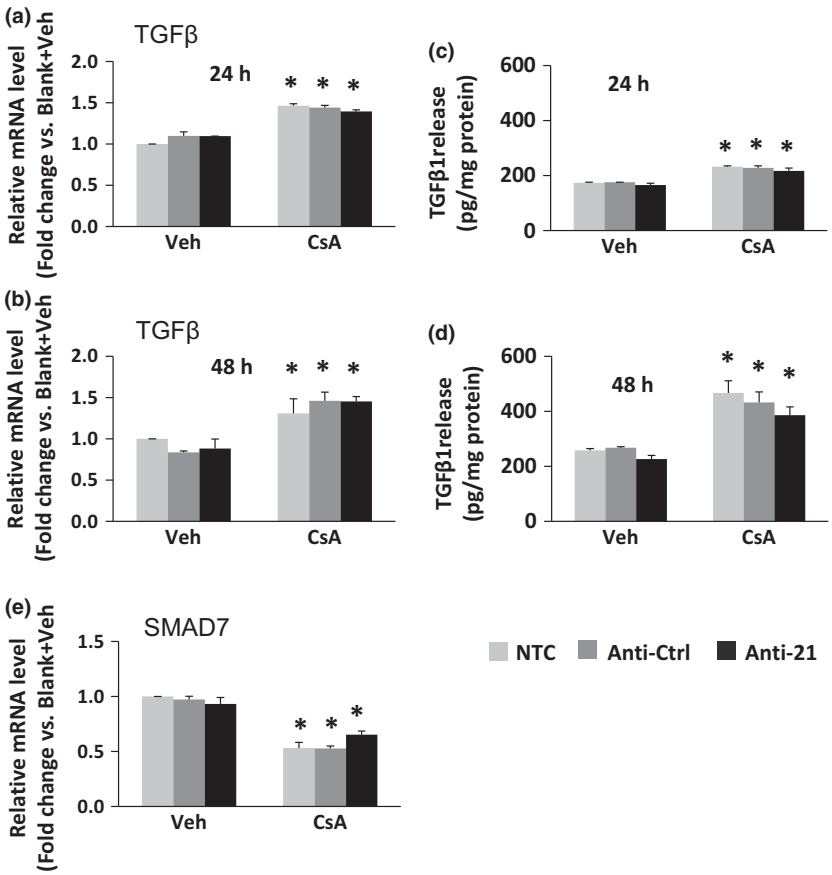

Figure 8 Inhibition of miR-21 did not alter CsA-induced TGF-β1 gene or protein expression and SMAD7 expression. PTECs were transfected with miR-21 inhibitor (Anti-21) or negative control of inhibitor miRNA (Anti-Ctrl) for 24 h, followed by 6 μM CsA treatment for 24 or 48 h. A nontransfected control (NTC) is shown for comparison. TGF-β1 mRNA expression at 24 h (a) and 48 h (b) is unaffected by Anti-21 treatment. TGF-β1 mRNA expression levels were analyzed using real-time PCR and shown as mean ± SEM of fold change. Anti-21 did not change CsA-induced increase of released TGF-β1 protein levels at 24 h (c) and 48 h (d). Released TGF-β1 protein levels were measured using specific TGF-β1 ELISA kit. The values were normalized to total protein level in same media. Results are shown as mean ± SEM of three independent experiments. (e) SMAD7 suppression by CsA is not affected by miR-21 inhibition. SMAD7 was measured by real-time PCR and shown as mean ± SEM of fold change. *$P < 0.05$ compared to corresponding vehicle treatment.

and miR-21. We chose to focus on miR-21 as recent studies have implicated miR-21 in regulating fibrosis in a number of organs and models. For example, in a mouse model of cardiac hypertrophy, Thum *et al.* [12] demonstrated that miR-21 is enriched in cardiac fibroblasts and augments the MAPK signaling, promoting fibroblast survival and growth factor secretion while inhibition of miR-21 reduced MAPK activity and interstitial fibrosis with improved cardiac function. In the kidney, unilateral urinary obstruction results in an inflammatory injury with renal dysfunction and upregulation of miR-21 expression primarily in the tubular epithelial cells and blockade of miR-21 attenuated the resulting fibrosis [14]. These studies again support the notion that miR-21 is a key control mechanism in tissue fibrosis.

Our focus on human renal proximal tubular epithelium was based on prior studies of CNI injury [26,49]. While EMT as a contributor to fibrosis *in vivo* remains debated [50,51], prior studies of CNI injury have supported CsA-induced EMT of tubular cells as contributing to renal fibrogenesis [18–20,27,28]. In this regard, we focused on the CsA-induced mesenchymal phenotypic changes in PTECs as a key site of molecular regulation of injury. Indeed, we demonstrate that in a model of chronic injury following exposure to CsA, miR-21 expression correlates with the development of injury. Moreover, a reduction in EMT-associated molecules in cultured cells follows blockade of miR-21, suggesting a novel strategy to mitigate CNI toxicity *in vivo*. Importantly, *in situ* detection of miR-21 following CsA toxicity shows dramatic expression throughout the kidney in a variety of cells both in cortex and medulla within the epithelium of the kidney. These findings precede the development of fibrosis, in contrast to those of Glowacki where the highest level of expression was seen with severe fibrosis [8]. However, a complicating feature of that

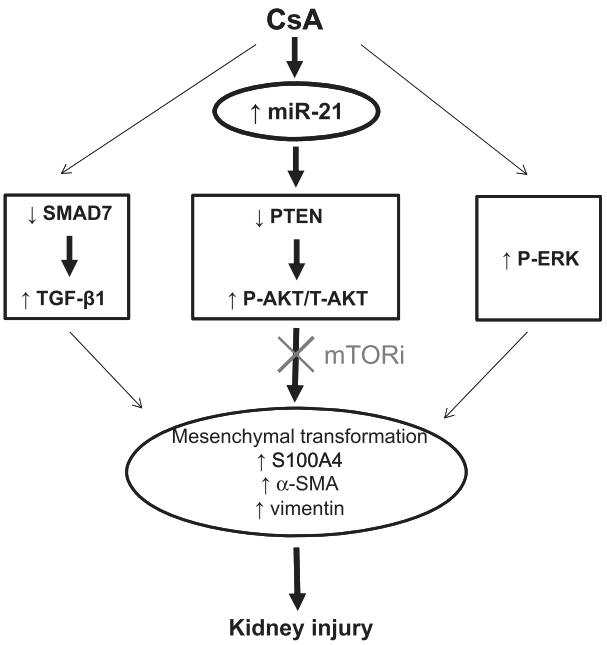

Figure 9 Proposed miR-21-mediated signaling leading to epithelial–mesenchymal transformation (EMT) in PTECs and kidney injury following CsA exposure. Three signaling pathways have been identified for miR-21 that could that result in mesenchymal transformation with induction of S100A4, α-SMA, or vimentin. However, following exposure of human PTECs to CsA, signaling through miR-21 primarily results in PTEN suppression and activation of AKT, independent of the effects on TGF-β signaling or ERK phosphorylation. Abrogation of this pathway could be clinically pertinent with the use of mTOR inhibition to mitigate the subsequent induction of genes and proteins associated with cell growth and differentiation.

study is the concomitant use of CNI throughout the patient course. Our results implicate an even wider potential for CsA-mediated injury by miR-21 than previously appreciated, as a potential indicator of occult damage prior to fully manifested injury.

The cell signaling pathways affected by miR-21 continue to be understood and are dependent on cell type and origin. In cardiac fibroblasts, miR-21 regulates the ERK–MAP kinase signaling pathway through inhibition of sprouty homologue 1 (Spry1), leading to their activation [12]. However, in lung fibroblasts, increased miR-21 levels promoted the pro-fibrogenic activity of TGF-β1 in lung fibroblasts through downregulating the expression of an inhibitory SMAD7 [11]. This pathway is biologically sensible as prior studies have demonstrated that TGF-β induces EMT [36,52,53] and promotes interstitial fibrosis by regulating matrix molecule production [54,55]. While we detect signaling via SMAD7/TGF-β following CsA exposure as previously reported [28], this pathway is not mediated by miR-21. Rather, our study demonstrates a new link with PTEN suppression and increased AKT phosphorylation in the kidney (Fig. 9). Furthermore, inhibition of miR-21 reduced CsA-induced AKT phosphorylation. This is not a global inhibition to other CsA-mediated signaling pathways, as inhibition of miR-21 did not affect CsA-induced upregulation of ERK phosphorylation.

Our results are consistent with other reports of miR-21-linked PTEN suppression as seen in cardiac fibroblasts following ischemic injury [1] and in hepatocellular carcinoma [31]. As an antagonist of phosphatidylinositol 3-kinase (PI3K), PTEN attenuates signaling molecules downstream of PI3K [56] and negatively regulates EMT through antagonism of the PI3K/AKT pathway [57,58]. While we demonstrate an association of miR-21 with AKT/PTEN signaling, we must be cautious and consider that miR-21 could target other mRNAs in hPTECs that are involved in modulating EMT. Further examination of these networks is warranted. Finally, our work suggests a potential explanation for the beneficial effects of mTORi in human kidney transplant recipients in long-term graft function [59] above and beyond the reduction or avoidance of CNI use via the PTEN pathway (Fig. 9).

A critical concern with our studies is the specificity of responses and potential for clinical application. The broad induction of miRNAs by CsA is not unexpected based on the current literature in other disease states [44]. Further, a single miRNA may regulate a wide variety of responses such that direct inhibition may lead to other unexpected effects of the treatment [4]. The demonstration that overexpression of miR-21 is associated with induction of the EMT markers in cultured cells but not entirely to the level of CsA alone suggests that this pathway is critical but doesn't exclude other contributory pathways. This is similarly supported by the incomplete abrogation of EMT gene expression with the anti-miR-21. This latter finding may also be due to our inability to completely inhibit miR-21 with the anti-mRNA transfection technique. The function of this inhibitor is unlike responses using siRNA, in which the expression of the miRNA is not affected but is functionally blocked. It is also conceivable that other miRNAs are induced that have overlapping functions in mediating mesenchymal changes, although miR-21 has been the most often studied.

The ability to avoid nephrotoxicity in the context of effective immunosuppression remains a critical issue in transplantation [60]. While TGF-β has been a focus of a number of studies as a key pro-fibrotic growth factor, its immunoregulatory properties limits its utility in transplant settings. Identifying tissue-specific targets is thus a critical task. The use of miRNAs as targets may be ideal, as there is clear tissue specificity of expression and signaling pathways as noted in this study. Blockade is feasible as demonstrated by preclinical studies, although these are

short-term exposures that may not be relevant to the human condition. Finally, although we have focused on miR-21, our data indicate other miRNAs with significantly altered expression following CsA exposure. These pathways may have additional contributions to nephrotoxicity and further investigation into the mechanism of their responses may warrant an approach of multiple blockades. This strategy may provide a new avenue to effectively treat CsA nephrotoxicity.

Authorship

JC and RBM: conceived and designed the study and analyzed the data. DZ: analyzed the data. JC and AZ: performed the experiments. JC and RBM: authored the manuscript.

Funding

This study was funded by the University of Alabama at Birmingham.

References

1. Roy S, Khanna S, Hussain SR, *et al.* MicroRNA expression in response to murine myocardial infarction: miR-21 regulates fibroblast metalloprotease-2 via phosphatase and tensin homologue. *Cardiovasc Res* 2009; **82**: 21.
2. Stefani G, Slack FJ. Small non-coding RNAs in animal development. *Nat Rev Mol Cell Biol* 2008; **9**: 219.
3. Ebert MS, Sharp PA. Roles for microRNAs in conferring robustness to biological processes. *Cell* 2012; **149**: 515.
4. Bartel DP. MicroRNAs: genomics, biogenesis, mechanism, and function. *Cell* 2004; **116**: 281.
5. Harfe BD. MicroRNAs in vertebrate development. *Curr Opin Genet Dev* 2005; **15**: 410.
6. Farid WR, Verhoeven CJ, de Jonge J, Metselaar HJ, Kazemier G, van der Laan LJ. The ins and outs of MicroRNAs as biomarkers in liver disease and transplantation. *Transpl Int* 2014; Jun 25. doi: 10.1111/tri.12379. [Epub ahead of print]
7. Ben-Dov IZ, Muthukumar T, Morozov P, Mueller FB, Tuschl T, Suthanthiran M. MicroRNA sequence profiles of human kidney allografts with or without tubulointerstitial fibrosis. *Transplantation* 2012; **94**: 1086.
8. Glowacki F, Savary G, Gnemmi V, *et al.* Increased circulating miR-21 levels are associated with kidney fibrosis. *PLoS ONE* 2013; **8**(2): e58014. doi: 10.1371/journal.pone.0058014
9. Godwin JG, Ge X, Stephan K, Jurisch A, Tullius SG, Iacomini J. Identification of a microRNA signature of renal ischemia reperfusion injury. *Proc Natl Acad Sci USA* 2010; **107**: 14339.
10. Cho JH, Gelinas R, Wang K, Etheridge A, Piper MG, Batte K, *et al.* Systems biology of interstitial lung diseases: integration of mRNA and microRNA expression changes. *BMC Med Genomics* 2011; **4**: 8.
11. Liu G, Friggeri A, Yang Y, *et al.* miR-21 mediates fibrogenic activation of pulmonary fibroblasts and lung fibrosis. *J Exp Med* 2010; **207**: 1589.
12. Thum T, Gross C, Fiedler J, *et al.* MicroRNA-21 contributes to myocardial disease by stimulating MAP kinase signalling in fibroblasts. *Nature* 2008; **456**: 980.
13. Yamada M, Kubo H, Ota C, *et al.* The increase of microRNA-21 during lung fibrosis and its contribution to epithelial-mesenchymal transition in pulmonary epithelial cells. *Respir Res* 2013; **14**: 95.
14. Zarjou A, Yang S, Abraham E, Agarwal A, Liu G. Identification of a microRNA signature in renal fibrosis: role of miR-21. *Am J Physiol Renal Physiol* 2011; **301**: F793.
15. Oak SR, Murray L, Herath A, *et al.* A micro RNA processing defect in rapidly progressing idiopathic pulmonary fibrosis. *PLoS One* 2011; **6**: e21253.
16. Andoh TF, Bennett WM. Chronic cyclosporine nephrotoxicity. *Curr Opin Nephrol Hypertens* 1998; **7**: 265.
17. Jiang T, Acosta D. An in vitro model of cyclosporine-induced nephrotoxicity. *Fundam Appl Toxicol* 1993; **20**: 486.
18. Hazzan M, Hertig A, Buob D, *et al.* Epithelial-to-mesenchymal transition predicts cyclosporine nephrotoxicity in renal transplant recipients. *J Am Soc Nephrol* 2011; **22**: 1375.
19. Martin-Martin N, Ryan G, McMorrow T, Ryan MP. Sirolimus and cyclosporine A alter barrier function in renal proximal tubular cells through stimulation of ERK1/2 signaling and claudin-1 expression. *Am J Physiol Renal Physiol* 2010; **298**: F672.
20. Naesens M, Kuypers DR, Sarwal M. Calcineurin inhibitor nephrotoxicity. *Clin J Am Soc Nephrol* 2009; **4**: 481.
21. Wang S, Zhang ZX, Yin Z, *et al.* Anti-IL-2 receptor antibody decreases cytokine-induced apoptosis of human renal tubular epithelial cells (TEC). *Nephrol Dial Transplant* 2011; **26**: 2144.
22. Andoh TF, Lam TT, Lindsley J, Alpers CE, Bennett WM. Enhancement of chronic cyclosporine nephrotoxicity by sodum depeltion in an experimental mouse model. *Nephrology* 1997; **3**: 471.
23. Young BA, Burdmann EA, Johnson RJ, *et al.* Cyclosporine A induced arteriolopathy in a rat model of chronic cyclosporine nephropathy. *Kidney Int* 1995; **48**: 431.
24. Yang CW, Faulkner GR, Wahba IM, *et al.* Expression of apoptosis-related genes in chronic cyclosporine nephrotoxicity in mice. *Am J Transplant* 2002; **2**: 391.
25. Jorgensen S, Baker A, Moller S, Nielsen BS. Robust one-day in situ hybridization protocol for detection of microRNAs in paraffin samples using LNA probes. *Methods* 2010; **52**: 375.
26. Pallet N, Bouvier N, Bendjallabah A, *et al.* Cyclosporine-induced endoplasmic reticulum stress triggers tubular phenotypic changes and death. *Am J Transplant* 2008; **8**: 2283.
27. Slattery C, Campbell E, McMorrow T, Ryan MP. Cyclosporine A-induced renal fibrosis: a role for epithelial-mesenchymal transition. *Am J Pathol* 2005; **167**: 395.
28. McMorrow T, Gaffney MM, Slattery C, Campbell E, Ryan MP. Cyclosporine A induced epithelial-mesenchymal transi-

tion in human renal proximal tubular epithelial cells. *Nephrol Dial Transplant* 2005; **20**: 2215.
29. Porter GA, Andoh TF, Bennett WM. An animal model of chronic cyclosporine nephrotoxicity. *Ren Fail* 1999; **21**: 365.
30. Porter GA, Bennett WM. Chronic cyclosporine-associated nephrotoxicity. *Transplant Proc* 1986; **18**(2 Suppl. 1): 204.
31. Meng F, Henson R, Wehbe-Janek H, Ghoshal K, Jacob ST, Patel T. MicroRNA-21 regulates expression of the PTEN tumor suppressor gene in human hepatocellular cancer. *Gastroenterology* 2007; **133**: 647.
32. Vinciguerra M, Sgroi A, Veyrat-Durebex C, Rubbia-Brandt L, Buhler LH, Foti M. Unsaturated fatty acids inhibit the expression of tumor suppressor phosphatase and tensin homolog (PTEN) via microRNA-21 up-regulation in hepatocytes. *Hepatology* 2009; **49**: 1176.
33. Zhang JG, Wang JJ, Zhao F, Liu Q, Jiang K, Yang GH. MicroRNA-21 (miR-21) represses tumor suppressor PTEN and promotes growth and invasion in non-small cell lung cancer (NSCLC). *Clin Chim Acta* 2010; **411**: 846.
34. Liang M, Liu Y, Mladinov D, *et al.* MicroRNA: a new frontier in kidney and blood pressure research. *Am J Physiol Renal Physiol* 2009; **297**: F553.
35. Lorenzen JM, Haller H, Thum T. MicroRNAs as mediators and therapeutic targets in chronic kidney disease. *Nat Rev Nephrol* 2011; **7**: 286.
36. Yeh YC, Wei WC, Wang YK, Lin SC, Sung JM, Tang MJ. Transforming growth factor-β1 induces Smad3-dependent β1 integrin gene expression in epithelial-to-mesenchymal transition during chronic tubulointerstitial fibrosis. *Am J Pathol* 2010; **177**: 1743.
37. Du MR, Zhou WH, Yan FT, *et al.* Cyclosporine A induces titin expression via MAPK/ERK signalling and improves proliferative and invasive potential of human trophoblast cells. *Hum Reprod* 2007; **22**: 2528.
38. O'Connell S, Tuite N, Slattery C, Ryan MP, McMorrow T. Cyclosporine A–induced oxidative stress in human renal mesangial cells: a role for ERK 1/2 MAPK signaling. *Toxicol Sci* 2012; **126**: 101.
39. Djamali A, Reese S, Hafez O, *et al.* Nox2 is a mediator of chronic CsA nephrotoxicity. *Am J Transplant* 2012; **12**: 1997.
40. Campistol JM, Inigo P, Larios S, Bescos M, Oppenheimer F. Role of transforming growth factor-beta1 in the progression of chronic allograft nephropathy. *Nephrol Dial Transplant* 2001; **16**(Suppl. 1): 114.
41. Lan HY. Diverse roles of TGF-beta/Smads in renal fibrosis and inflammation. *Int J Biol Sci* 2011; **7**: 1056.
42. Zhong X, Chung AC, Chen HY, Meng XM, Lan HY. Smad3-mediated upregulation of miR-21 promotes renal fibrosis. *J Am Soc Nephrol* 2011; **22**: 1668.
43. Jevnikar AM, Mannon RB. Late kidney allograft loss: what we know about it, and what we can do about it. *Clin J Am Soc Nephrol* 2008; **3**(Suppl. 2): S56.
44. Bhatt K, Mi QS, Dong Z. microRNAs in kidneys: biogenesis, regulation, and pathophysiological roles. *Am J Physiol Renal Physiol* 2011; **300**: F602.
45. Wei L, Wang M, Qu X, *et al.* Differential expression of microRNAs during allograft rejection. *Am J Transplant* 2012; **12**: 1113.
46. Anglicheau D, Sharma VK, Ding R, *et al.* MicroRNA expression profiles predictive of human renal allograft status. *Proc Natl Acad Sci USA* 2009; **106**: 5330.
47. Scian MJ, Maluf DG, David KG, *et al.* MicroRNA profiles in allograft tissues and paired urines associate with chronic allograft dysfunction with IF/TA. *Am J Transplant* 2011; **11**: 2110.
48. Shapiro MD, Bagley J, Latz J, *et al.* MicroRNA expression data reveals a signature of kidney damage following ischemia reperfusion injury. *PLoS One* 2011; **6**: e23011.
49. Bakker RC, van Kooten C, van de Lagemaat-Paape ME, Daha MR, Paul LC. Renal tubular epithelial cell death and cyclosporin A. *Nephrol Dial Transplant* 2002; **17**: 1181.
50. Liu Y. New insights into epithelial-mesenchymal transition in kidney fibrosis. *J Am Soc Nephrol* 2010; **21**: 212.
51. Fragiadaki M, Mason RM. Epithelial-mesenchymal transition in renal fibrosis - evidence for and against. *Int J Exp Pathol* 2011; **92**: 143.
52. Iwano M. EMT and TGF-beta in renal fibrosis. *Front Biosci (Schol Ed)* 2010; **2**: 229.
53. Kong W, Yang H, He L, *et al.* MicroRNA-155 is regulated by the transforming growth factor beta/Smad pathway and contributes to epithelial cell plasticity by targeting RhoA. *Mol Cell Biol* 2008; **28**: 6773.
54. Border WA, Noble NA. Transforming growth factor beta in tissue fibrosis. *N Engl J Med* 1994; **331**: 1286.
55. Wolf G. Renal injury due to renin-angiotensin-aldosterone system activation of the transforming growth factor-beta pathway. *Kidney Int* 2006; **70**: 1914.
56. Rosivatz E. Inhibiting PTEN. *Biochem Soc Trans* 2007; **2**: 257.
57. Wang H, Quah SY, Dong JM, Manser E, Tang JP, Zeng Q. PRL-3 down-regulates PTEN expression and signals through PI3K to promote epithelial-mesenchymal transition. *Cancer Res* 2007; **67**: 2922.
58. Yao Y, Wei H, Liu L, *et al.* Upregulated DJ-1 promotes renal tubular EMT by suppressing cytoplasmic PTEN expression and Akt activation. *J Huazhong Univ Sci Technolog Med Sci* 2011; **31**: 469.
59. Geissler EK, Schlitt HJ. The potential benefits of rapamycin on renal function, tolerance, fibrosis, and malignancy following transplantation. *Kidney Int* 2010; **78**: 1075.
60. Mannon RB. Therapeutic targets in the treatment of allograft fibrosis. *Am J Transplant* 2006; **6**: 867.